High-temperature quenching of electrical resistance in graphene interconnects

Q. Shao, G. Liu, D. Teweldebrhan, and A. A. Balandin[a)]
Nano-Device Laboratory, Department of Electrical Engineering, University of California-Riverside, Riverside, California 92521, USA and Materials Science and Engineering Program, Bourns College of Engineering, University of California-Riverside, Riverside, California 92521, USA

(Received 14 April 2008; accepted 23 April 2008; published online 19 May 2008)

The authors reported on the experimental investigation of the high-temperature electrical resistance of graphene. The test structures were fabricated by using the focused ion beam from the single and bilayer graphene produced by mechanical exfoliation. It was found that as temperature increases from 300 to 500 K, the resistance of the single, and bilayer graphene interconnects drops down by 30% and 70%, respectively. The quenching and temperature dependence of the resistance were explained by the thermal generation of the electron-hole pairs and carrier scattering by acoustic phonons. The obtained results are important for the proposed graphene interconnect applications in integrated circuits. © *2008 American Institute of Physics*. [DOI: 10.1063/1.2927371]

As the electronic industry aggressively moves toward nanometer designs, thermal issues are becoming increasingly important for the high-end electronic chips. The integrated circuit performance is now limited by the maximum power, which can be dissipated without exceeding the maximum junction temperature setup by the reliability requirements.[1,2] According to the International Technology Roadmap for Semiconductors (ITRS) projections, the volumetric heat generation rates within interconnects will be approaching $P=j^2\rho\sim 3.3\times 10^4\ \mathrm{W/mm^3}$ assuming a current density $j=3.9\ \mathrm{MA/cm^2}$ and a resistivity $\rho=2.2\ \mu\Omega\ \mathrm{cm}$. The self-heating problem is aggravated by the increased integration densities, faster clock speed, high dissipation power density in interconnect networks, increased total thermal boundary resistance of the chip layers, incorporation of the alternative dielectric materials with low thermal conductivity values, as well as acoustic phonon confinement effects in nanometer scale structures.[3,4]

One of the approaches to mitigate the self-heating problem is to incorporate into the chip interconnect design the materials with low electrical resistance and high thermal conductivity. Carbon nanotubes have been considered for interconnects in the very large scale integrated (VLSI) circuit applications.[5,6] Graphene, a form of carbon consisting of separate atomic planes of sp^2-bound atoms,[7] was also proposed for the interconnect applications.[8,9] Graphene manifests extremely high room temperature (RT) electron mobility as high as $\sim 15\,000\ \mathrm{cm^2\,V^{-1}\,s^{-1}}$. It was recently reported by Balandin *et al.*[10,11] that graphene is also a superior heat conductor with the RT thermal conductivity in the range of 3100–5300 W/mK.[10,11] The latter adds validity to the proposed interconnect applications of graphene, owing to potential benefit for thermal management. In this case, graphene interconnects may be used for high-heat flux cooling and help with lateral heat spreading and hot-spot removal. Since conventional VLSI circuits operate at elevated temperatures (100–200 K above RT), it is important to understand how the electrical resistance of graphene interconnects changes as the temperature increases from 300 to 500 K.

In this letter, we show that the electrical resistance of graphene, which is a semimetal with zero band gap,[7] undergoes strong quenching as the temperature exceeds RT. Interestingly, this behavior is opposite to that manifested by some technologically important bulk semimetals such as bismuth telluride or related alloys widely used in thermoelectrics.[12] We have produced a large number of graphene layers by mechanical exfoliation from the bulk highly oriented pyrolitic graphite (HOPG) and from the high-pressure high-temperature (HPHT) grown material.[13] The single-layer graphene (SLG) and bilayer graphene (BLG) were found with the help of micro-Raman spectroscopy through the two-dimensional (2D)-band deconvolution procedure.[14–16]

Raman spectra were measured at RT using a Renishaw instrument under 488 nm excitation wavelength in the backscattering configuration.[15,16] Figure 1 shows the characteristic Raman spectrum with a clearly distinguishable *G* peak

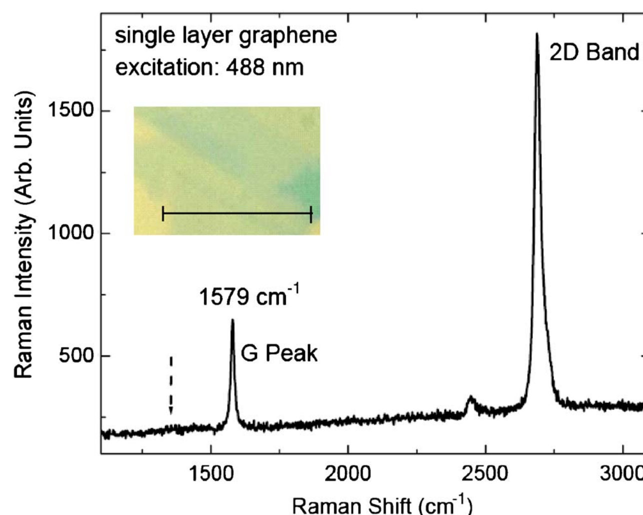

FIG. 1. (Color online) Raman spectrum of the graphene flake, which was used for the interconnect fabrication. The position of *G* peak and the spectral features of the 2D band confirm the number of atomic layers. Inset shows optical image of HPHT graphene used for the sample preparation. Light-green areas correspond to SGL; the scale bar is 5 μm.

[a)]Author to whom correspondence should be addressed. Electronic mail: balandin@ee.ucr.edu. URL: http://ndl.ee.ucr.edu.

 © 2008 American Institute of Physics
Author complimentary copy. Redistribution subject to AIP license or copyright, see http://apl.aip.org/apl/copyright.jsp

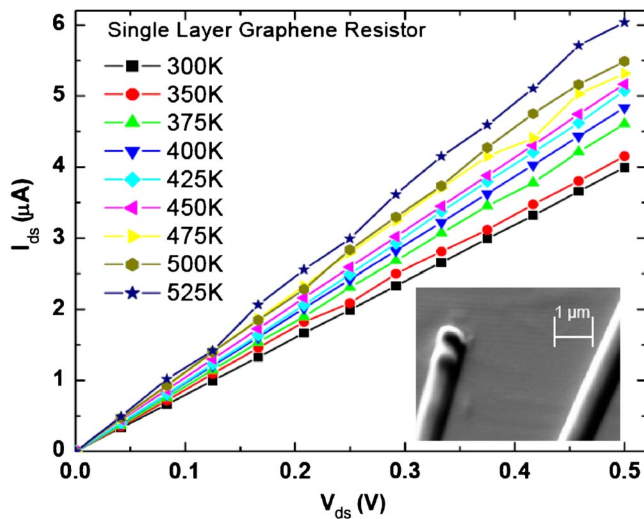

FIG. 2. (Color online) High-temperature current-voltage characteristics of graphene resistors. Inset shows the SEM image of the graphene interconnects contacted through FIB-fabricated platinum electrodes.

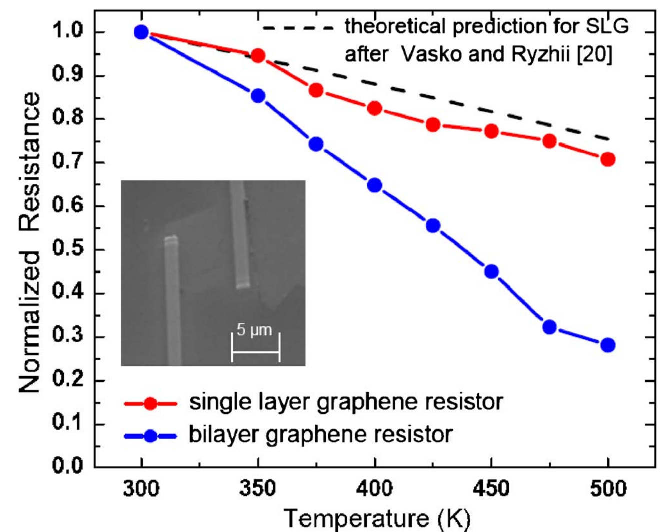

FIG. 3. (Color online) Normalized electrical resistance of SLG and BLG interconnects as a function of temperature. The theoretical prediction for SLG from Ref. 20 is shown for comparison. Note a strong quenching of the resistance at temperatures above RT. Inset shows a close up SEM image of BLG resistors between two electrodes.

and 2D band. The position of the G peak and shape of the 2D band confirm that the examined flake is SLG. The disorder-induced D peak is absent in the scattering spectra from a HPHT graphene (its expected position is indicated by an arrow), which suggests a high quality of SLG material. Graphene layers have been transferred to Si substrates with the electrically insulating oxide films of thickness $W \geqslant 0.3\ \mu$m grown on top of them. A set of SLG and BLG resistors contacted by platinum (Pt) electrodes have been fabricated using the Leo XB1540 focused ion beam (FIB) system. The absence of leakage current through the oxide layer was verified by applying a very high bias (up to $\sim$20 V) between the top electrodes and back gate (metallization on the back side of the Si substrate) and ensuring that the resulting current is negligibly small.

The graphene resistors between two metal electrodes on an insulating oxide layer, which can be considered as prototype graphene interconnects, have been electrically characterized in the temperature range $T=300-500$ K. The temperature was controlled externally through the Signatone probe-station hot chuck. In Fig. 2, we present typical current-voltage (I-V) characteristics for the SLG interconnect fabricated from a HOPG material. The inset shows a scanning electron microscopy (SEM) image of the SLG resistor between two Pt electrodes. The electrical properties of interconnects made of HOPG and HPHT graphenes were similar for the examined set of samples. As one can see, the resistors are ohmic and the current increases with increasing temperature. Such a behavior is a characteristic for intrinsic semiconductors where the electrical conductivity σ_i obeys the following temperature dependence[17] $\sigma_I \sim \exp[-\Delta E_i/(2k_BT)]$ (here, ΔE_i is the band gap and k_B is the Boltzmann's constant). The decreasing resistance of semiconductors with T is due to the growing concentration of the thermally generated electron-hole pairs. It is influenced by the band gap renormalization and carrier scattering on phonons as the temperature changes.[17]

It is interesting to note that the measured trend in graphene is the opposite to that in bulk semimetals of bismuth type (e.g., Bi_xSb_{1-x}, Bi–Ti, Bi–Sn), where resistivity ρ follows the law[12] $\rho=\rho_o+AT$ (here, A is a positive constant between $(2.3-14)\times 10^{-7}\ \Omega\,\text{cm/K}$). Such dependence for semimetals and metals is explained by the increasing electron-phonon scattering at elevated temperature.[18] In metals, the number of charge carriers does not change with temperature but the interaction with phonons increases. The latter results in the temperature dependence of the type $R=R_0[1+\alpha(T-T_0)]$, where α is the temperature coefficient of resistance. At low temperature, resistance is limited by impurities, which leads to increasing mobility and decreasing resistance with T. The temperature dependence of resistance in bismuth near RT reverses when one makes a nanostructure out of it, e.g., nanowire, with the lateral dimensions below some critical value. In this case, a semimetal-semiconductor transition is induced by quantum confinement, which results in the experimentally observed change in the resistance temperature dependence.[19]

Figure 3 presents the electrical resistance for SLG and BLG interconnects as a function of temperature. The resistances were normalized to their values at RT for better comparison. The plot also shows a theoretical curve for the SLG resistor obtained from the model recently proposed by Vasko and Ryzhii[20] and renormalized to RT value for better comparison. Our experimentally obtained dependence for SLG is in excellent agreement with the calculations. According to the theory proposed in Ref. 20, the decrease in resistance at RT and above comes from the thermal generation of carriers while the values and shape of the resistance curve are determined by electron and hole scattering on the long and short range disorder and acoustic phonons. Cheianov and Falko[21] also predicted a negative linear T dependence of resistivity $R(T)$ in graphene described by the expression $R(T)=R(0)-(h/e^2)(4TV_0/hv^2E_F\tau_o)$, where h is the Plank's constant, e is the charge of an electron, E_F is the Fermi energy, τ_0 is a backscattering rate from atomically sharp defects in graphene lattice, which does not include Coulomb scatterers, v is the velocity, and V_0 is a characteristic interaction constant.[21] For our samples, we obtained the following linear analytical approximation for the high-temperature normalized resistance of SLG: $R(T)/R(T=300\text{ K})=1.436$

Author complimentary copy. Redistribution subject to AIP license or copyright, see http://apl.aip.org/apl/copyright.jsp

$-0.00147T$. From the known characteristic velocity in graphene of $V_F \sim 10^8$ cm/s and the experimentally determined temperature when the resistance quenching sets up ($\sim$300–350 K), we can estimate the correlation length for the disorder scattering in our graphene resistors,[20] i.e., $l_c \sim V_F h/(2\pi T k_B)$, to be around 22–25 nm. The origin of the difference in the resistance temperature dependence for SLG and BLG requires further theoretical and experimental investigation. One should note here that the data in Ref. 20 was plotted for maximum R near the neutrality point while Ref. 21 considered the "heavily doped" case.

It is illustrative to compare electrical resistance of graphene with that of bulk graphite and other carbon materials. It was known for a long time that single graphite crystals are good electrical conductors along the graphite planes and very poor ones across with the ratio of resistivities above $\sim 10^4$.[22] There is a substantial discrepancy for the reported temperature dependence of the electrical resistance in bulk graphite, which likely can be attributed to the variations in the material quality. From the data presented in Refs. 23 and 24, the resistance decreases with increasing temperature around RT, although in one case, the decrease is sublinear, while in another case, it is superlinear. The high-temperature resistance decreases with temperature in the coke base carbon (T=300–800 K) and graphitized lampblack base carbon (T=300–2000 K) as summarized in Ref. 25, although the dependence is very different from what we have measured for graphene. In some types of carbon, e.g., graphitized coke base carbon, the decreasing trend reverses to increasing resistivity around 400–500 K.[25]

In conclusion, we experimentally investigated the high-temperature electrical resistance of graphene single and bilayer conductors. It was found that as the temperature increases from 300 to 500 K, the resistance of the single and BLG interconnects drops substantially. In this sense, despite being semimetal with zero band gap, graphene resistors behave more like intrinsic semiconductors. The high-temperature normalized resistance of SLG resistor can be approximated as $R(T)/R(T=300\text{ K}) = 1.436 - 0.00147T$. The observed resistance quenching in graphene resistors may have important implications for the proposed applications in interconnects and thermal management. The resistance quenching in the relevant temperature range (100–200 K above RT) by 30%–70% may lead to a significant reduction in power dissipation.

This work was supported, in part, by DARPA-SRC through the FCRP Interconnect Focus Center (IFC), AFOSR through award A9550-08-1-0100 on Electron and Phonon Engineered Nano- and Heterostructures and DARPA-DMEA through the UCR-UCLA-UCSB Center for Nanoscience Innovations for Defense (CNID). A.A.B. thanks Dr. E.P. Pokatilov, D.L. Nika (Moldova State Univ), Dr. N. Kalugin (New Mexico Tech), and Dr. F.T. Vasko (Inst of Semiconductor Physics) for critical reading of the original manuscript and Dr. A.G. Fedorov (Georgia Tech) for illuminating discussions on interconnects.

[1] A. Vassighi and M. Sachdev, *Thermal and Power Management of Integrated Circuits* (Springer, New York, 2005), Chap. 1.
[2] S. P. Gurrum, S. K. Suman, Y. K. Joshi, and A. G. Fedorov, IEEE Trans. Device Mater. Reliab. **4**, 709 (2004); Y. Joshi, K. Azar, D. Blackburn, C. J. M. Lasance, R. Mahajan, and J. Rantala, Microelectron. J. **34**, 1195 (2003).
[3] A. A. Balandin and K. L. Wang, Phys. Rev. B **58**, 1544 (1998); A. A. Balandin, E. P. Pokatilov, and D. L. Nika, J. Nanoelectron. Optoelectron. **2**, 140 (2007).
[4] E. P. Pokatilov, D. L. Nika, and A. A. Balandin, Phys. Rev. B **72**, 113311 (2005); J. Superlattices and Microstruct. **38**, 168 (2005).
[5] N. Srivastava and K. Banerjee, *Proceedings of the 2005 IEEE/ACM International Conference on Computer-Aided Design* (IEEE, Washington DC, 2005), pp. 383–390.
[6] Q. Ngo, A. M. Cassell, A. J. Austin, J. Li, S. Krishnan, M. Meyyappan, and C. Y. Yang, IEEE Electron Device Lett. **27**, 221 (2006); Q. Ngo, B. A. Cruden, A. M. Cassell, G. Sims, M. Meyyappan, J. Li, and C. Y. Yang, Nano Lett. **4**, 2403 (2004).
[7] A. K. Geim and K. S. Novoselov, Nat. Mater. **6**, 183 (2007).
[8] A. Naeemi and J. D. Meindl, IEEE Electron Device Lett. **28**, 428 (2007).
[9] S. Hong, Y. Yoon, and J. Guo, Appl. Phys. Lett. **92**, 083107 (2008).
[10] A. A. Balandin, S. Ghosh, W. Bao, I. Calizo, D. Teweldebrhan, F. Miao, and C. N. Lau, Nano Lett. **8**, 902 (2008).
[11] S. Ghosh, I. Calizo, D. Teweldebrhan, E. P. Pokatilov, D. L. Nika, A. A. Balandin, W. Bao, F. Miao, and C. N. Lau, Appl. Phys. Lett. **92**, 151911 (2008).
[12] G. Kuka, W. Kraak, H.-J. Gollnest, and R. Herrmann, Phys. Status Solidi B **89**, 547 (1978).
[13] F. Parvizi, D. Teweldebrhan, S. Ghosh, I. Calizo, A. A. Balandin, H. Zhu, and R. Abbaschian, Micro & Nano Lett. **3**, 29 (2008).
[14] A. C. Ferrari, J. C. Meyer, V. Scardaci, C. Casiraghi, M. Lazzeri, F. Mauri, S. Piscanec, D. Jiang, K. S. Novoselov, S. Roth, and A. K. Geim, Phys. Rev. Lett. **97**, 187401 (2006).
[15] I. Calizo, F. Miao, W. Bao, C. N. Lau, and A. A. Balandin, Appl. Phys. Lett. **91**, 071913 (2007); I. Calizo, W. Bao, F. Miao, C. N. Lau, and A. A. Balandin, Appl. Phys. Lett. **91**, 201904 (2007).
[16] I. Calizo, D. Teweldebrhan, W. Bao, F. Miao, C. N. Lau, and A. A. Balandin, J. Phys.: Condens. Matter **109**, 012008 (2008); I. Calizo, A. A. Balandin, W. Bao, F. Miao, and C. N. Lau, Nano Lett. **7**, 2645 (2007).
[17] G. Busch and H. Schade, *Lectures on Solid State Physics* (Pergamon, New York, 1976), p. 289.
[18] A. Seeger and K. Clausecker, Phys. Status Solidi B **46**, 137 (1971).
[19] D. S. Choi, A. A. Balandin, M. S. Leung, G. Stupian, N. Presser, S. W. Chung, J. R. Heath, A. Khitun, and K. L. Wang, Appl. Phys. Lett. **89**, 141503 (2006).
[20] F. T. Vasko and V. Ryzhii, Phys. Rev. B **76**, 233404 (2007).
[21] V. V. Cheianov and V. I. Fal'ko, Phys. Rev. Lett. **97**, 226801 (2006).
[22] S. Mrozowski, Phys. Rev. **77**, 838 (1950).
[23] J. M. Reynolds, H. W. Hemstreet, and T. E. Leinhardt, Phys. Rev. **91**, 1152 (1953).
[24] J. M. Skowronski, Carbon **26**, 613 (1988).
[25] *Standard Handbook for Electrical Engineers* (McGraw-Hill, New York, 1993), pp. 4–84.

Author complimentary copy. Redistribution subject to AIP license or copyright, see http://apl.aip.org/apl/copyright.jsp